Adhesive and TIG Joining Nickel-Titanium to 304 Stainless Steel

Undergraduate Honors Thesis

Presented in Partial Fulfillment of the Requirements for

Graduation with Honors Research Distinction

at The Ohio State University

By

Mark Riggs

* * * * *

The Ohio State University

2012

Defense Committee:

Advisor: Dr. Marcelo Dapino

Dr. Amos Gilat

Approved by:

Advisor

Undergraduate Program in
Mechanical Engineering

ABSTRACT

Nickel-titanium (NiTi) contains a unique set of properties which make it a desirable candidate for aeronautic applications. NiTi's most useful characteristic comes from being a Shape Memory Alloy (SMA). With the proper thermo-mechanical training regimen, a NiTi tube can generate high stress as it rotates through large amounts of strain based on a thermal triggering condition. The rotation cycle is controlled by the temperature of the alloy and it is fully recoverable with up to 8% strain. This rotation lends itself well to function as a solid state actuator. Solid state actuators are beneficial over the traditional hydraulic or electrical actuators because they show the potential to be small, lightweight, and survive harsh conditions. Despite these advantages, NiTi has limitations, including poor machinability. This project looks into testing different methods of joining NiTi with structural materials to enable system integration. Once NiTi can be consistently joined with a machineable material its application will become more practical. This project investigates different ways to join Nickel-Titanium with structural materials to accelerate system integration.

ACKNOWLEDGEMENTS

Personal

I would like to express my appreciation to Professor Marcelo Dapino for supporting me in my research. His guidance has been crucial, and I cannot fully show the admiration I have for Dr. Dapino's support.

I would also like to thank the students in the Smart Material and Structures Lab. All of the fellow research students have been understanding and patient with questions concerning the lab. In particular I would like to thank Gordon Fox for his previous work and his guidance as he patiently passed on knowledge about the project. I would also like to thank Ryan Hahnlen and Ben Thornton for their input.

Project

The NiTi joining project began in January 2008 in the Smart Vehicle Concepts Center, a National Science Foundation center at The Ohio State University and Texas A&M University. Boeing has served as the main sponsor and the Edison Welding institute (EWI) has served as a collaborator. The project was started by Ryan Hahnlen as the lead graduate student and later taken over by Gordon Fox. In October of 2011 the author began working side by side with Gordon and took over the project in April of 2012. The work described below is not intended to be all encompassing for the project. However, background information performed by the previous students is given to allow a basis for the work done by the author. The majority of the work performed by the author is the second set of adhesive tests and the continuation of Tungsten Inert Gas welding tests.

TABLE OF CONTENTS

Contents

LIST OF FIGURES

LIST OF TABLES

CHAPTER 1: INTRODUCTION

1.1 Shape Memory Alloys

A Shape Memory Alloy (SMA) has the ability to undergo large amounts of deformation while maintaining the ability to return to its original shape. It can undergo deformation with two elastic regions coupled by a transition region between two martensitic structures. These two structures are twinned and detwinned martensite. Once the twinned martensite has sustained its maximum shear stress, the structure begins to transition into detwinned martensite with the formation of dislocations until the detwinned structure is fully formed. Figure 2 visually illustrates the transition from twinned to detwinned martensite under shear loading and Figure 2 shows the two elastic regions on a stress vs. strain plot.

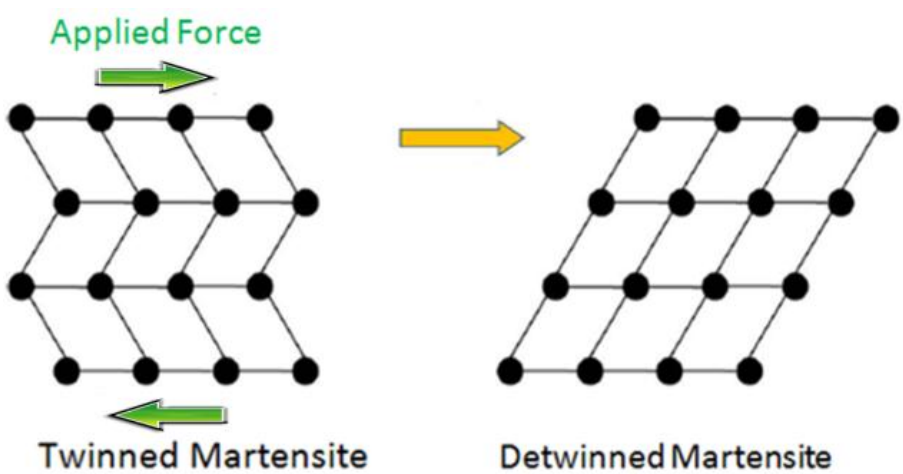

Figure 1: Transition from Twinned to Detwinned Martensite

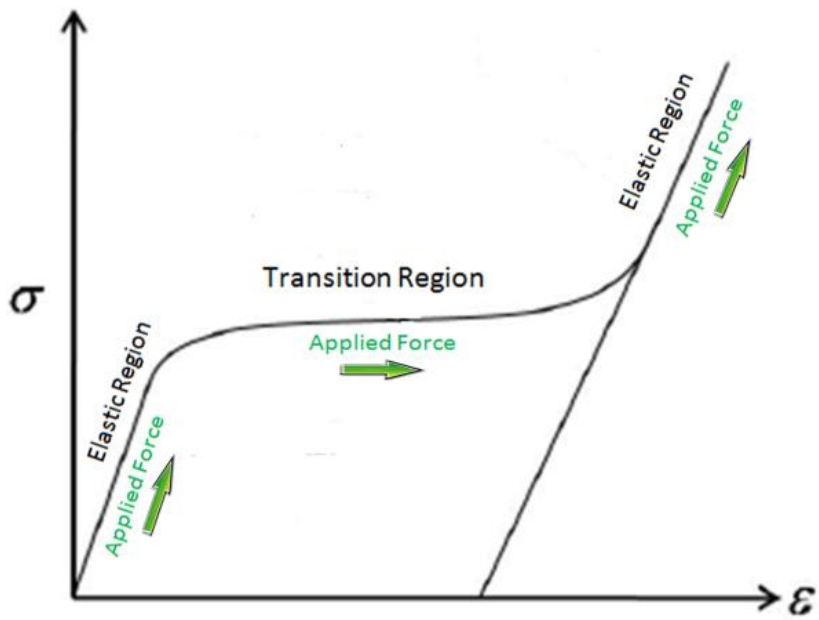

Figure 2: Transition from Twinned to Detwinned Martensite Stress vs. Strain

Once the load is removed the elastic deformation is recovered, but the transition deformation remains. This unrecovered deformation is seemingly plastic, but it is recoverable by heating the SMA. Shape memory alloys can not only change from twinned martensite to detwinned martensite, but they can also change to a third crystalline structure, austenite. The transition from either martensite form to austenite is accomplished through changing the temperature of the alloy.

Four stress dependent temperatures dictate the crystalline structure within the SMA. The volume fraction of martensite is a parameter used to describe the martensite-austenite ratio (ξ) within the SMA. If the alloy is fully martensitic, $\xi=1$, its temperature is below the martensite finish temperature. As the material is heated past the austenite start temperature the material structure begins to form austenite with the martensite volume fraction decreasing. When the SMA's temperature is above the austenite finish temperature the material is in its austenite form, $\xi=0$. The material has now fully transformed from martensite to austenite based on temperature

changes. The reverse is true from austenite to martensite with a martensite start temperature and a cooler martensite finish temperature. Figure 3 is a generic plot of the volume fraction of martensite against the four key temperatures [3]. Exact values for the temperatures are not given; the transition temperatures depend upon stress and the composition of the alloy.

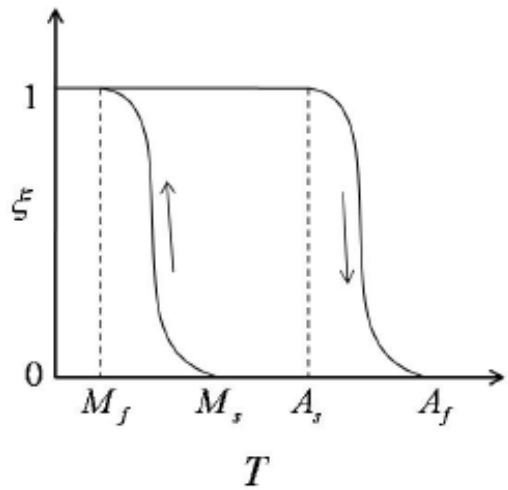

Figure 3: Volume fraction of Martensite vs. Temperature

The change from martensite to austenite transitions the molecular structure back to its original length. Once the material is in its austenitic structure it has recovered all of the previous deflection. Figure 4 shows the corresponding molecular structure for the transformation.

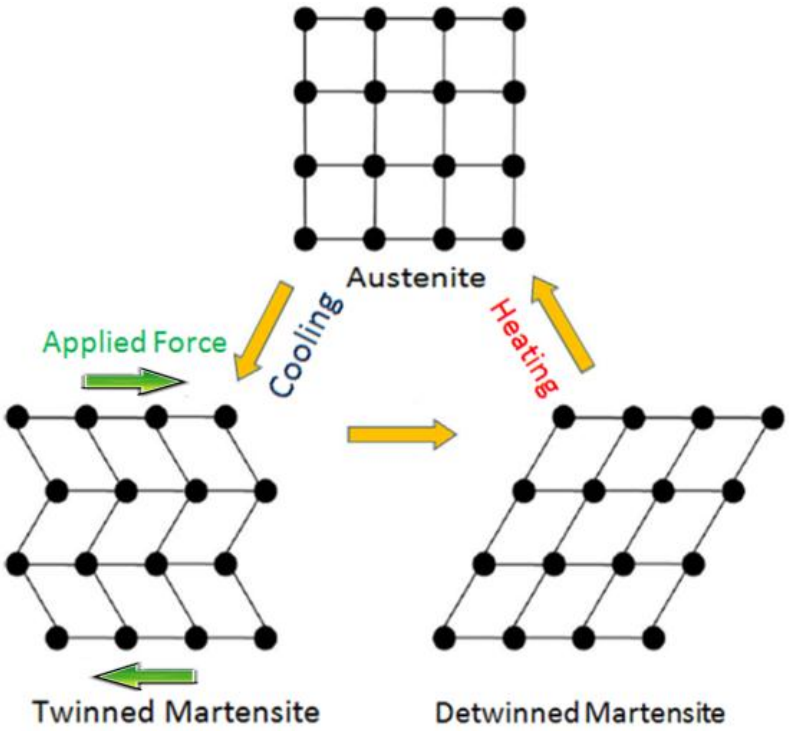

Figure 4: Full One Way Shape Memory Transition

Cooling the austenitic material past its martensite finish temperature returns the alloy to its original state. This transformation occurs at the origin of the stress vs. strain diagram if the cooling is performed without an applied stress and the length does not change. This process is shown in Figure 4 and it is referred to as the one way shape memory effect.

Shape memory alloys with a one way shape memory effect are capable of remembering their austenitic length, but "forget" their deformed length caused by the applied load. It is desirable to have an SMA that remembers both lengths based on a thermal trigger. This is possible through a thermo-mechanical training regimen. After the alloy is trained it exhibits what is called a two way shape memory effect. The two way shape memory effect changes from its original austenitic length to a "remembered" length because of a developed preferential orientation in the martensitic phase. The NiTi tubes used for testing in this project have been trained to have the two way shape memory effect with rotation about its longitudinal axis.

1.2 NiTi Characteristics

Nearly equi-atomic nickel titanium (NiTi) is a shape memory alloy which is capable of being trained to have a two way shape memory effect. It is a strong SMA candidate for multiple reasons. NiTi is capable of recovering strains of up to 8% while generating high amounts of stress. The transition temperatures are easy to work with because of their proximity to room temperature. NiTi is less expensive than other SMAs. NiTi also has a high ultimate shear strength of over 120 ksi (960 MPa), at which point the deformation becomes plastic. These are all properties that make NiTi the alloy of choice for a solid state actuator. While NiTi has its advantages, it also has its drawbacks. The primary disadvantage of NiTi is its poor machinability due to its high ductility. This makes machining bolts and splines difficult and expensive with high amounts of tool wear [4].

1.3 Industrial Applications

The NiTi tubes used in this project have a two way shape memory effect which allows the material to remember both the austenitic length and a trained deformation length in the martensite phase. This results in the ability to change the SMA's length based on temperature. If the alloy is below the martensite finish temperature it is at the deformed length, and if the alloy is above the austenitic finish temperature it is at the original length. Additionally, the deformation has been observed to occur under the application of a load because of the generated internal stress associated with the preferential orientation [5]. This implies that the SMA can produce useful work in the form of an actuator.

The type of the work done by a SMA is dictated by the thermo-mechanical training regimen. The training regimen used for the NiTi tubes in this project creates a rotation about the longitudinal axis. The tubes rotate without changing length or cross sectional area. This actuation

has been used by Boeing to experiment with controlling the twist profile of rotor blades with "on-the-fly" control. The goal is to use a trained NiTi tube inside of the spare to twist the blade from an optimal hover angle to an optimum forward flight configuration at the pilot's command [5]. The test stand used for this application can be seen in Figure 5.

Figure 5: "On-the-Fly" Rotary Blade Control

Another experimental application of NiTi used by Boeing is seen in the actuation of chevrons in the exhaust stream of an aircraft engine. NiTi bars are passively actuated by the ambient temperature to change the chevron's geometry. When the plane is on the runway the ambient temperature is high enough to actuate the NiTi bars and reduce noise. In flight the temperature at cruising altitude is low enough to retract the chevrons and reduce drag. This technology is called a Variable Geometry Chevron and the application can be seen in Figure 6.

Figure 6: Boeing Variable Geometry Chevron

1.4 Motivation

While Boeing has implemented Shape Memory Alloys into their innovative designs, widespread implementation of NiTi has been hindered by its poor machinability. The major shortcoming of NiTi is its expense and complexity in system integration. However, if the NiTi is joined with a structural material, such as Aluminum 2024 or stainless steel 304 (304 SS), the structural material can be machined to enable the integration of the smart system to the surrounding structures. The concept of system integration is the basis for joining NiTi to structural materials in order to help take advantage of applications such as “On-the-Fly” rotary blade control and Variable Geometry Chevrons.

1.5 Joining Methods

Several methods of joining NiTi to structural materials have been experimentally investigated. Among those are laser welding, ultrasonic soldering, adhesives and tungsten inert gas (TIG) welding. The joining methods of interest for this project are adhesives and TIG welding. Descriptions of these joining processes follow.

1.5.1 Adhesive Joints

Adhesives utilize a specialized film between two surfaces that bond the surfaces together. This is a low temperature process, which prevents a possible loss of training in the SMA caused by excessive heat. Adhesives are a very familiar process throughout the aerospace industry and their strength can be increased by increasing the bond area. Adhesives are a proven technology and testing their application in conjunction with NiTi is desired. The adhesive being used is Hysol EA9696 SOT Grade 10, which was formulated by Boeing [2].

Adhesives have been tested at The Ohio State University in a first round of experimental testing. The joints were made with the EA9696 and EA 9394 adhesives with a NiTi tube being bonded into a split Al 2024 block. The diagram of the adhesive joint is shown in Figure 7 along with a constructed joint. The first round of testing focused on the effects of temperature, bond depth, and grip type on the ultimate failure torque. The results from this test showed that temperature significantly impacts the strength of the joint, bond depth increases the ultimate failure torque, and grip type between split and solid blocks has no statistical significance. The tests also showed that the newer EA9696 is stronger than the old EA9394 counterpart. This information was used in preparing the second round of testing to determine the durability of the joint over time with a special interest in high temperature testing.

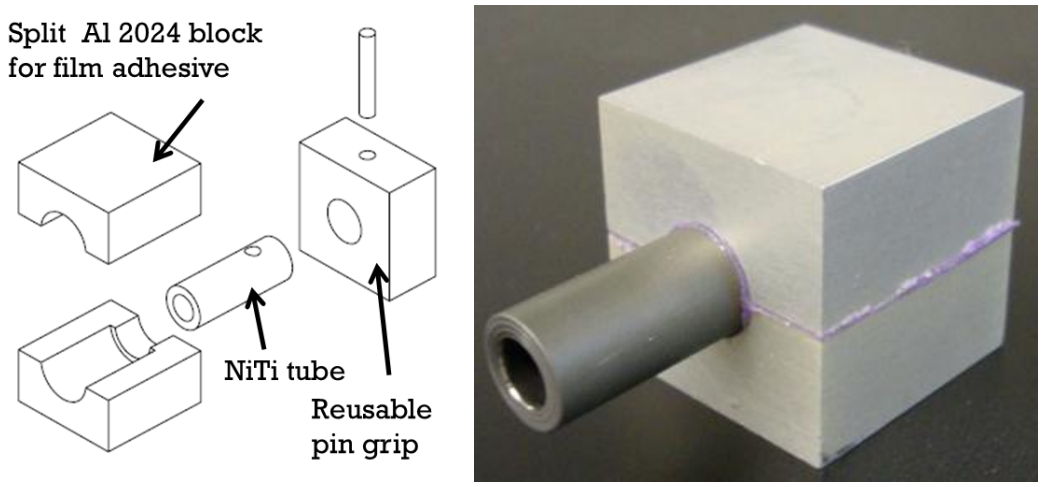

Figure 7: NiTi Adhesive Test Joint

1.5.2 Tungsten Inert Gas Welded Joints

The second joining method of focus uses a fusion welding process called Tungsten Inert Gas Welding (TIG). TIG welding uses an electric arc with a nonconsumable electrode to melt work pieces together as it is surrounded by a shielding gas, typically Argon, to prevent the formation of oxides. TIG welding is very well known in standard applications, but there are two challenges that make it difficult to apply with NiTi and ferrous alloys.

The first challenge is the formation of a heat affected zone. NiTi is sensitive to heat and that is part of what makes it useful as an SMA. However, excessive heat deteriorates its training through thermo-mechanical cycling. NiTi must be heated above 1300℃ (2400℉) to melt in the fusion welding process, but it begins to lose its shape memory effects above 500℃ (930℉). The size of the HAZ is important because the SMA's transformation characteristics are affected by heat [4].

The second challenge is the formation of cracks. Hot cracking is a result of Ni_2Ti being formed in the liquid state as the NiTi solidifies in the weld pool. The thermal stresses of cooling

create cracks in the Ni_2Ti which can propagate throughout the weld. The second form of cracking is cold cracking. If NiTi and a ferrous alloy are welded together the weld pool will mix titanium and iron together forming TiFe and $TiFe_2$ intermetallics. These intermetallics have a low strength at room temperature and are subject to thermal stresses caused by cooling. To help prevent the formation of brittle intermetallics, an Ni rich filler is used between the two metals [4]. This filler has been found to lower the chances of cracking and is employed in the TIG specimens used for testing.

The TIG welded specimens used in experiments have an outer diameter of 0.375" (9.5mm) and the wall thicknesses were left as received at 0.075" (1.91mm) and 0.065" (1.65mm) for the NiTi and 304 SS tubes, respectively. The geometries and configuration of the 304 SS and NiTi joint are shown in Figure 8 with a test joint shown in Figure 9.

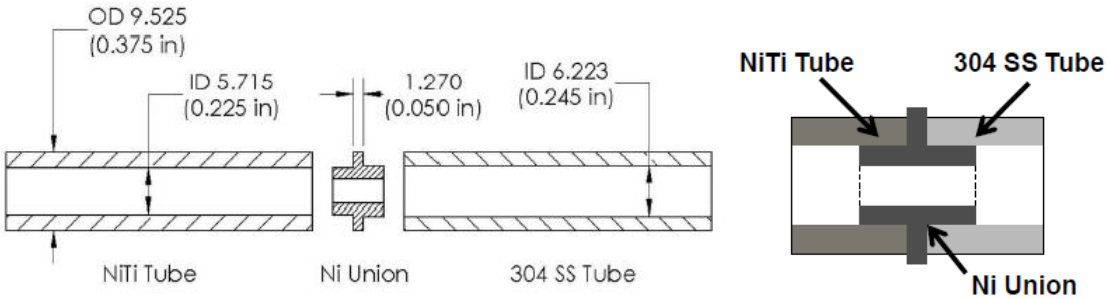

Figure 8: TIG Welded Specimen Configuration

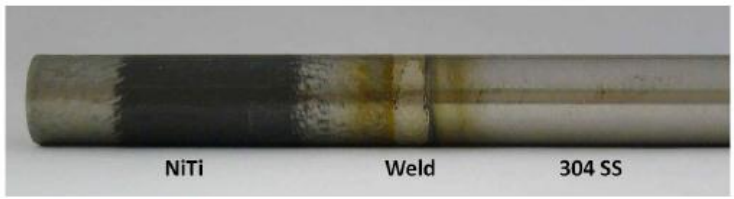

Figure 9: Experimental TIG Welded Specimen

CHAPTER 2: TESTING PROCESS

2.1 Testing Overview

The goal of testing experimental joints is to analyze their strength in multiple cases. The two primary controlled variables in testing are the torque and the temperature of the alloy. A known torque is necessary because the rotational actuators withstand a shear stress resulting from work performed in applications described in Section 1.3. The temperature of the alloy must be controlled to simulate thermal cycles and test the joint at two different operating conditions. Given these criteria, a high temperature torque testing machine was created to test the joints [4].

2.1 High Temperature Torque Testing Machine

The machine used to impart the torque and thermal cycling is the high temperature torque testing machine seen in Figure 10. Torque is applied to the specimen through a DC motor and gearbox. The limiting factor on the amount of torque applied to the specimen is the torque cell, which has a range from 0 to 500 in-lbs. The specimen is held by aluminum grips, shown in Figure 11, with the left grip fixed and the right grip free to rotate. The specimen is held within the grips by a pin connection in the right grip and a pin connection in the left grip for the TIG specimen, or a clamping force on the aluminum block for the adhesive joint.

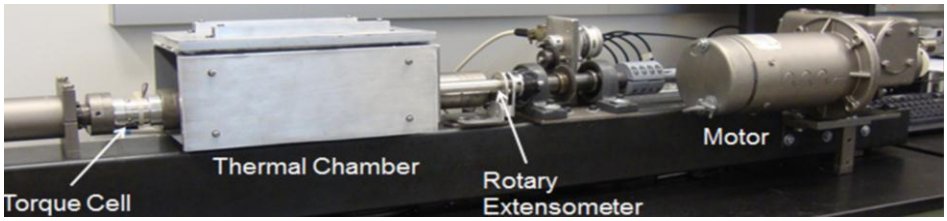

Figure 10: High Temperature Torque Testing Machine

While the torque is being applied, the temperature of the specimen is controlled within the thermal chamber. The specimen is heated with two cartridge heaters in both aluminum grips. The heaters are powered by a DC voltage controlled by Proportional Integral (PI) control. Vortex tubes are used to cool the specimen with a cutoff temperature of 25℃. To help facilitate heat transfer during the cooling cycle heat sinks are used in combination with the vortex tubes to allow for more surface area delivering higher cooling power. The temperature of the specimen is monitored on both sides with thermocouples threaded into the tube on either end.

The high temperature torque testing machine is also capable of measuring the angular deflection of the NiTi specimen. It is important to know the angular deflection in future analysis to decipher the effectiveness of the solid-state actuator. This measurement is taken with a rotary extensometer and an angular encoder. The rotary extensometer measures the difference in angular deflection relative to two points on the tube of the test specimen. The angular encoder measures the angular deflection of the specimen from grip to grip relative to the machine and the machine's stiffness.

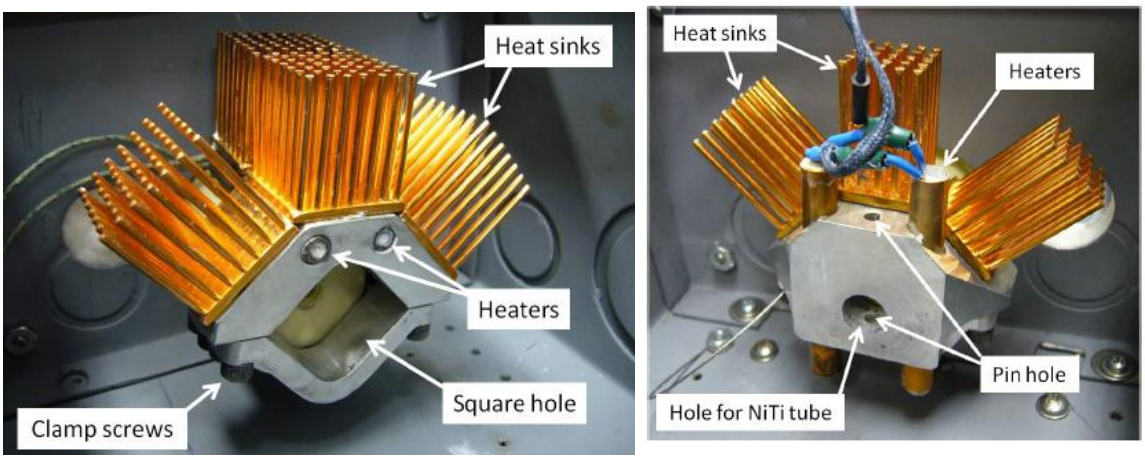

Figure 11: Specimen Grips

2.2 Types of Tests

Three primary tests are used for evaluation of the joints. These tests include the ultimate failure, creep, and thermal cycling. The ultimate failure test applies an increasing torque until the torque is no longer transmitted through the joint, which indicates failure. The ultimate failure test can be run at any temperature. The temperatures used for this project were room temperature (20°C) and an elevated temperature of 120°C. The creep test is an endurance test with a constant load being applied at a constant temperature. The load is either 50 or 75% of the ultimate failure torque and the temperature is either room temperature or 120°C. The thermal cycling test is performed in the same manner as the creep test, but the temperature is not held constant. Instead the temperature cycles between room temperature and 120°C. The thermal cycling transitions the crystalline structures and simulates actuation as a solid-state actuator.

2.3 Machine Improvements

The torque, temperature and angular deflection are the three primary quantities used to control and analyze the performance of the joint. Recently, the temperature acquisition system has been upgraded and in doing so corrected an electrical grounding issue associated with the thermal chamber. The previous thermocouples required a grounding wire to be fed through the thermal chamber and attached to the right grip. This was done in an effort to take away fluctuations in the temperature signal because of insufficient grounding. A major side effect to this simple fix was that the entire metal casing of the thermal chamber was connected to the electrical circuit through the grounding wire. The cartridge heater voltage supply came into electrical contact with the thermal chamber while trouble shooting a test. This sent a voltage through the thermal chamber and into the thermocouple chip. The voltage transmitted through the system of electrical contacts was sufficient to damage the thermocouple chip. The previous

thermocouple chip was also intended for surface mount applications and it was replaced with an AD594 chip. The new thermocouple chip has built in circuits for cold junction reference and required significantly fewer electrical connections. The thermocouples were calibrated with accuracy of $\pm 1°C$. The new thermocouple chips read temperatures accurately and effectively without the need for added grounding wires.

In addition to improving the reliability of the temperature measurement, the torque transfer mechanism within the grips was improved for endurance tests. The previous grips used thin aluminum shims to transfer the torque from the ceramic shafts to the grip. The friction caused by the aluminum shim and compressive forces by bolted junctions allow the torque to be transferred. However, the shim was a laminated peel-away aluminum shim. After an extended time at elevated temperature the lamination melted and the input shaft rotated relative to the aluminum grip. Figure 12 shows the shim stock peeling apart as the lamination melted. As a result the angular deflection readings were incorrect and misleadingly large. The laminated shim stock was replaced with pure aluminum shims to properly transmit the torque. With this correction the endurance tests can run properly while recording accurate angular deflection.

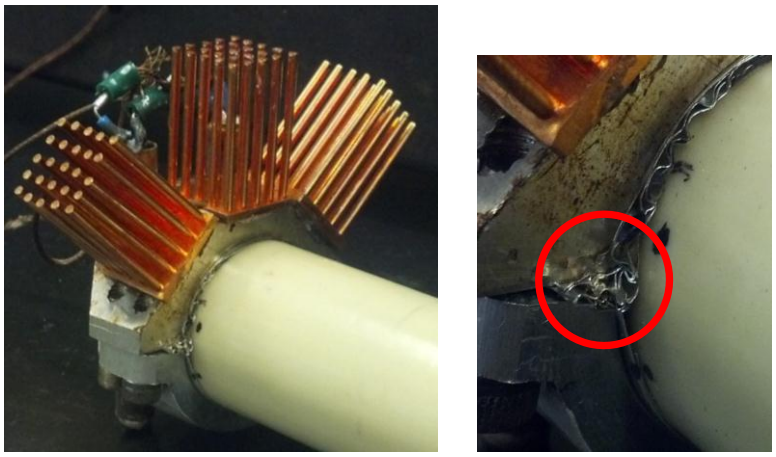

Figure 12: Laminated Shim Failure

CHAPTER 3: ADHESIVE JOINT TESTING

3.1 Test Matrix

The objective of the adhesive testing was to analyze how well the adhesive joints held up over time. This was accomplishes with a series of creep and thermal cycling tests.

The endurance tests were intended to test the durability of the joint. Because the joint is not desired to fail quickly, a proper load torque must be determined. Adhesive test specimens were tested for the ultimate failure torque and a percentage of this torque was used for the creep and thermal cycling tests. The creep test uses a constant torque at an elevated temperature of 120°C (250°F). The thermal cycling tests are under a constant torque with a cycling SMA temperature from 22°C (72°F) to 120°C (250°F). The test matrix for this round of adhesive tests is shown below in Table 1 [2].

Table 1: Adhesive Round 2 Test Matrix

	Test #	Load % of ultimate	Duration	Temperature °C (°F)	Replications
Ultimate failure	1	100	n/a	22 (72)	3
	2	100	n/a	120 (250)	3
Creep	3	50	24 hours	22 (72)	3
	4	50	24 hours	120 (250)	3
	5	75	24 hours	22 (72)	3
	6	75	24 hours	120 (250)	3
Thermal Cycling	7	50	Hundred of cycles or until failure	25 – 120 (77-250)	3
	8	75	Hundred of cycles or until failure	25 – 120 (77-250)	3
				Total	24

3.2 Test Results

The first adhesive tests performed were the ultimate failure tests. The adhesives performed well at high temperatures with an ultimate failure torque of 388.2 in-lbs which results in 6.67ksi of shear stress at the bonded joint. The room temperature test joints performed better than the high temperature tests with an average failure shear stress of 7.82ksi compared to 6.67ksi. It was expected that the elevated temperature tests would fail before the room temperature tests because of previous testing which confirmed that increased temperature degrades the joint strength [4].

An example plot of the high temperature torque vs. angle plots is shown below in Figure 13. Here it can be seen that the NiTi tube increases in angular deflection as the torque increases until the torque transfer in the system is lost because of joint failure. The loss of torque transfer is indicated by a sharp drop from high to low torque readings in the load cell. This peak torque is known as the breaking torque highlighted in Figure 13.

Of the two adhesive joints tested at room temperature neither joint failed under the increasing torque. The tests were both stopped by helical cracks formed at the pin hole connections. An example of a helical crack in an adhesive specimen is shown in Figure 14 and data from these tests can be seen in Table 2. The ultimate failure torque testing was completed and the endurance testing began with a creep test at elevated temperature [4].

The shear stresses in the NiTi tubes were approximated by finding the maximum shear stress in the tube by using the outer radius, torque and the bond depth. Equations i and ii show the relationships used to find the shear stress in the adhesive joints.

$$\tau = \frac{T/r}{A} \qquad (i)$$

$$Where: \tau = Shear\ Stress(psi), T = Torque(ksi), r = Outside\ tube\ radius\ (in)$$

$$and\ A = Surface\ Area\ of\ the\ adhesive\ bond$$

$$A = 2 * \pi * r * d \qquad (ii)$$

$$Where\ r = Outside\ tube\ radius\ (in), \qquad d = bond\ depth$$

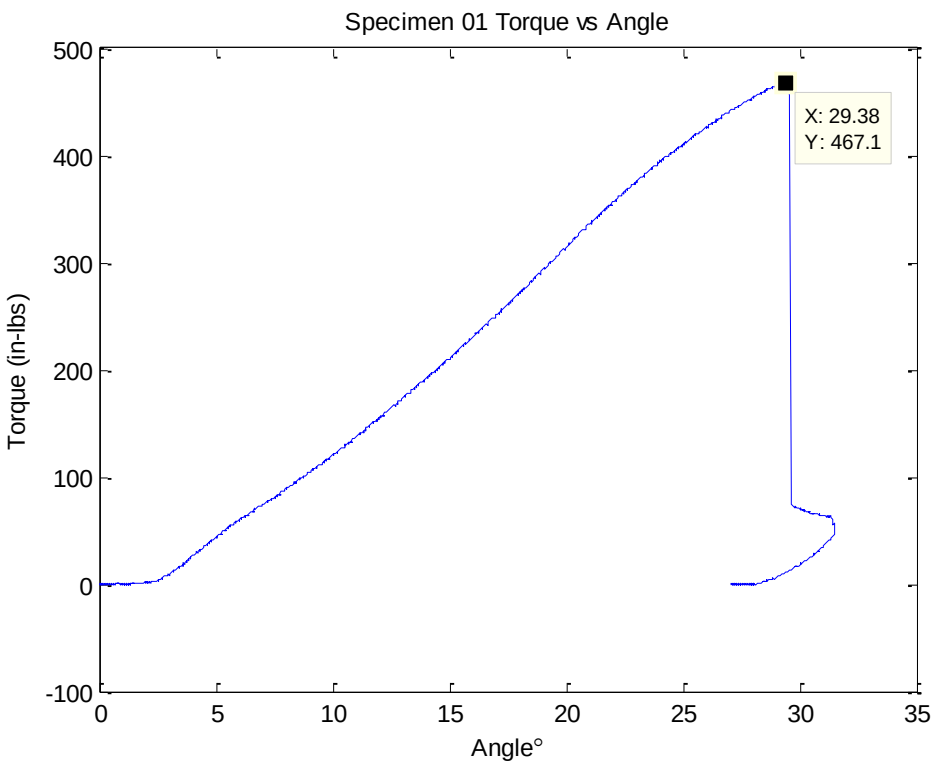

Figure 13: Specimen 01 Torque vs. Angle

Table 2: Adhesive Ultimate Failure Testing Data

Test Type	Temperature	Specimen #	Failing Point in-lb (Nm)	Average in-lb (Nm)	Shear Stress ksi (MPa)	Average (ksi)
Ultimate Failure Test	Elevated Temperature to 250°F (121°C)	01	467.1 (52.78)	388.2 σ=64.9 (43.86 σ=7.33)	8.02 (55.3)	6.67 σ=1.11 (46.0 σ=7.65)
		06	405.7 (45.84)		6.97 (48.)	
		07*	367.1 (41.48)		6.31 (43.5)	
		08	312.9 (35.35)		5.38 (37.1)	
	Room Temperature 70°F (21°C)	02	435.1 (49.16)**	455 σ=48.2 (51.41 σ=5.45)	7.47 (51.5)	7.82 σ=0.83 (53.9 σ=5.72)
		14	420 (47.45)** & 510 (57.62)**		7.22 (49.8) & 8.67 (60.4)	

*Heated for 30minutes at 110°C **Helical crack formed

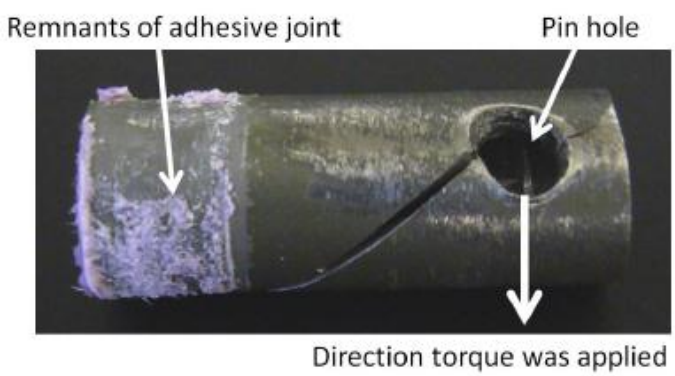

Figure 14: Helical Crack in Adhesive Pin Hole

The second set of experiments involved testing the endurance of the joints. Two tests were performed for creep at 50% of the ultimate failure torque at elevated temperature. As expected, the joints did not fail immediately and they were allowed to rest at elevated temperature with a constant load. However, the joints failed soon after the tests began. The

average life was on the order of minutes instead of hours or days. This was an unexpected result and there is no apparent reason for the failure relative to the adhesive joints used for ultimate failure testing.

Two tests were then performed under thermal cycling. Specimen 13 was expected to fail early because it had been improperly manufactured. The tube was slightly angled and the construction of the joint was not reasonably aligned. Specimen 5 passed the visual test and it was tested under thermal cycling with a constant load. This test lasted 3.5 thermal cycles, which spanned the time of 21.5 minutes. The angular deflection, shown in Figure 15, is seen to oscillate as the NiTi is transitioned between its martensite and austenite structures. However, the dominating trend is provided by the gradual joint degradation as the angular deflection consistently grows until failure. Before the results from the creep tests were observed the thermal cycling was expected to last on the order of a hundred cycles. The data can be seen in Table 3.

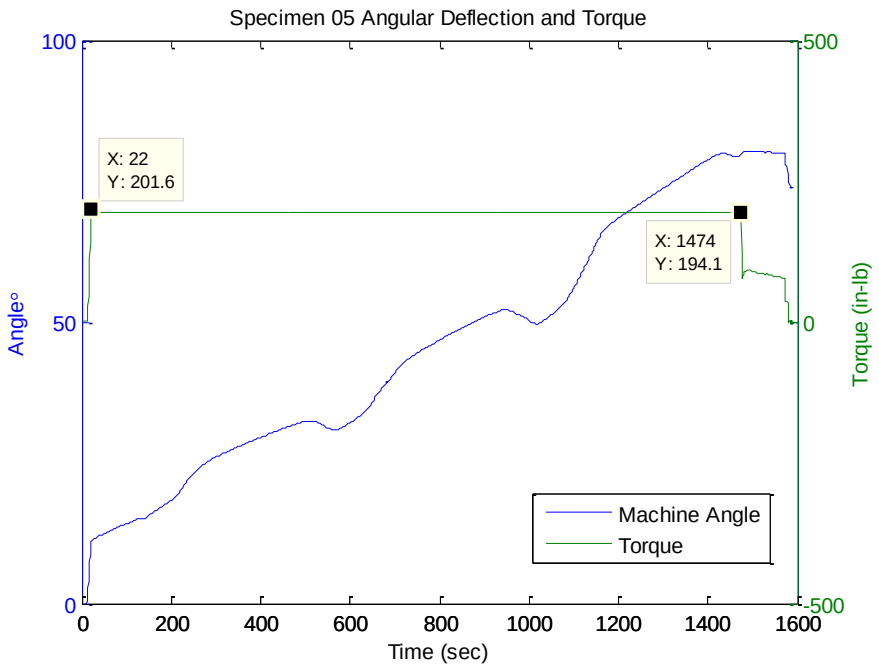

Figure 15: Angular Deflection and Torque for Specimen 05 during Thermal Cycling

Table 3: Adhesive Endurance Testing Data

Test Type	Specimen #	Temperature	Torque in-lb (Nm)	Shear Stress ksi (MPa)	Failing Point (Time or Cycles)
Creep Test	04	250°F (121°C)	50% UFTA 194.1 in-lb (21.9)	3.33 (23.0)	4 minutes
	03				8.5 minutes
Thermal Cycling	05	70 to 250°F (21 to 121°C)			3.5 cycles (21.5 minutes)
	13*				<1 cycle (2minutes)

*Improperly manufactured joint

3.3 Discussion

In order for a joining method to be effective it must last for an extended period of time at high temperature. It was known that the adhesive joints would be weaker at room temperature, but not by this magnitude. The specimens used for testing were selected at random and fabricated in the identical manner as the ultimate failure test specimens. Relative to the joints used in the ultimate failure tests, it is unknown why the joints failed soon after the torque was applied.

CHAPTER 4: TIG JOINT TESTING

4.1 Test Matrix

TIG testing was performed with thermal cycling and a constant load. Because of a limited supply of TIG joints to be tested, the ultimate failure results from previous testing were used instead of reproducing the data. The two TIG specimens were started at a low torque and increased to half of the ultimate failure torque of 453 in-lb [1]. This was done to avoid failure without recording several cycles. The first test used a more conservative cycling matrix with five thermal cycles being performed at each torque, seen in Table 4. The second and third tests were performed with less conservative regimens to gain more thermal cycles at half of the ultimate failure torque seen in Tables 5 and 6.

Table 4: TIG Specimen #1 First Test Matrix

Total Number of Cycles: 20		Average Cycle Time:	
Number of Cycles	Torque (in-lb)	Shear Stress (ksi)	Cycle Temperatures
5	45.1	5ksi	70F to 250F (25C to 121C)
5	135.1	15ksi	
5	181	20.1ksi	
5	226.5	25.1ksi	

Table 5: TIG Specimen #2 Test Matrix

Total Number of Cycles: 20		Average Cycle Time:	
Number of Cycles	Torque	Shear Stress	Cycle Temperatures
2	45.1	5ksi	70F to 250F (25C to 121C)
2	135.1	15ksi	
2	181	20.1ksi	
14	226.5	25.1ksi	

Table 6: TIG Specimen #1 Second Test Matrix

Total Number of Cycles: 20		Average Cycle Time:	
Number of Cycles	Torque	Shear Stress	Cycle Temperatures
2	45.1	5ksi	70F to 250F (25C to 121C)
2	135.1	15ksi	
2	181	20.1ksi	
14	226.5	25.1ksi	

4.2 Test Results

The TIG welds held up under all three tests with the TIG 1 weld being tested twice with a total of 40 cycles and the TIG 2 weld being tested once with a total of 20 cycles. During testing the joint was put under a constant torque while the NiTi was transitioned between its martensitic and austenitic phases. During the thermal cycling, the angular deflection changes as it transforms into its preferred martensitic orientation because of the thermo-mechanical training which created a two way shape memory effect.

For each test the controlled variables were the torque and the temperature of the SMA. The torque and the temperature plots are shown in Figure 16 for the second TIG1 Test which was the third test performed. For this test the toque was held constant at 45.1in-lbs for 2 cycles, 135.1 in-lbs for 2 cycles, 181 in-lbs for 2 cycles, and 226.5in-lbs for 14 cycles while the temperature cycled between 70°F and 250°F as seen before in Table 6. The thermal cycles induced structure transformations from martensite to austenite and the corresponding trained angular deflections occurred. Figure 17 shows the angular deflection as temperature is cycled along with the torque. In the fifth cycle, shown in Figure 16 and 17, the temperature does not elevate above the austenite start temperature and the angular deflection does not change as a result. This was the result of a hardware connection that was fixed immediately. The angle vs.

temperature plot is seen to oscillate between two geometries in Figure 18 and the torque is seen to have an effect on the angular deflection in Figure 19. As the torque increases the angular deflection increases because of the larger applied load.

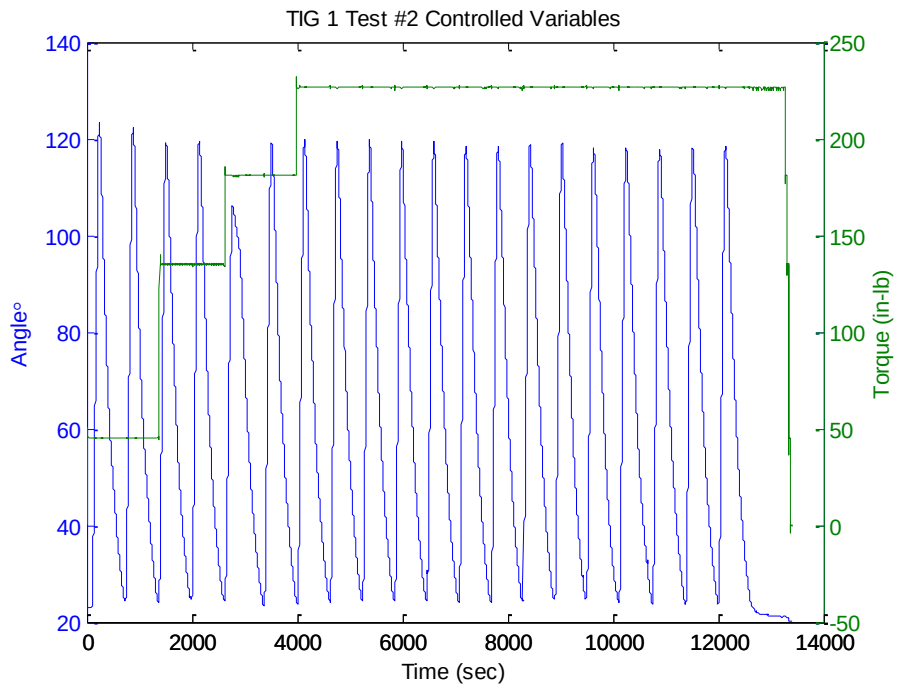

Figure 16: TIG 1 Test #2 Controlled Variables

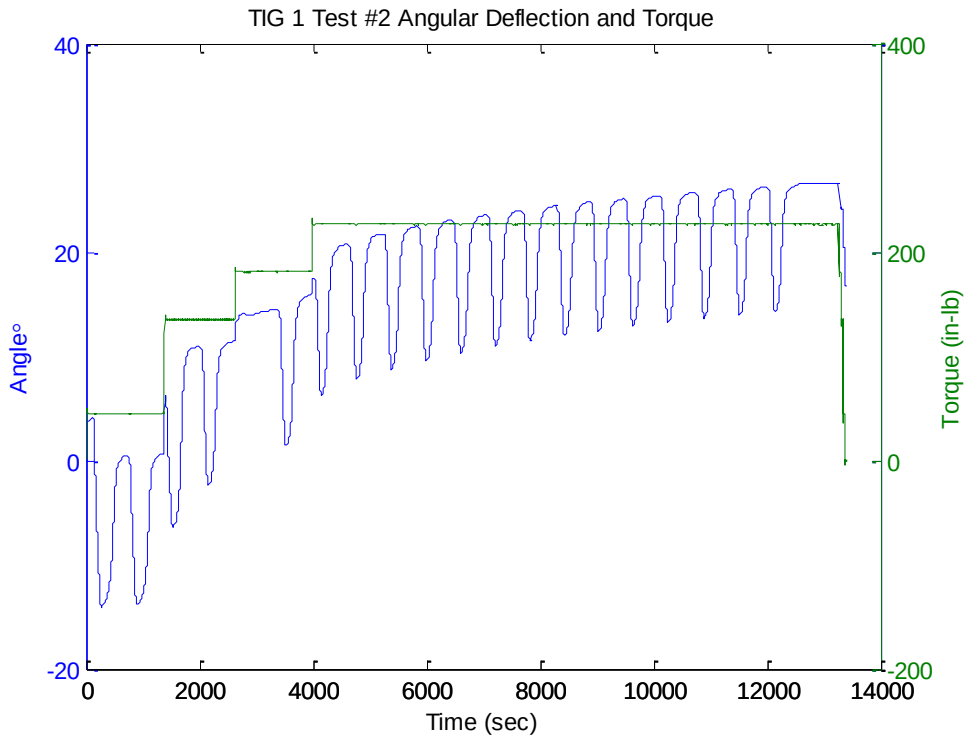

Figure 17: TIG 1 Test #2 Angular Deflection and Torque

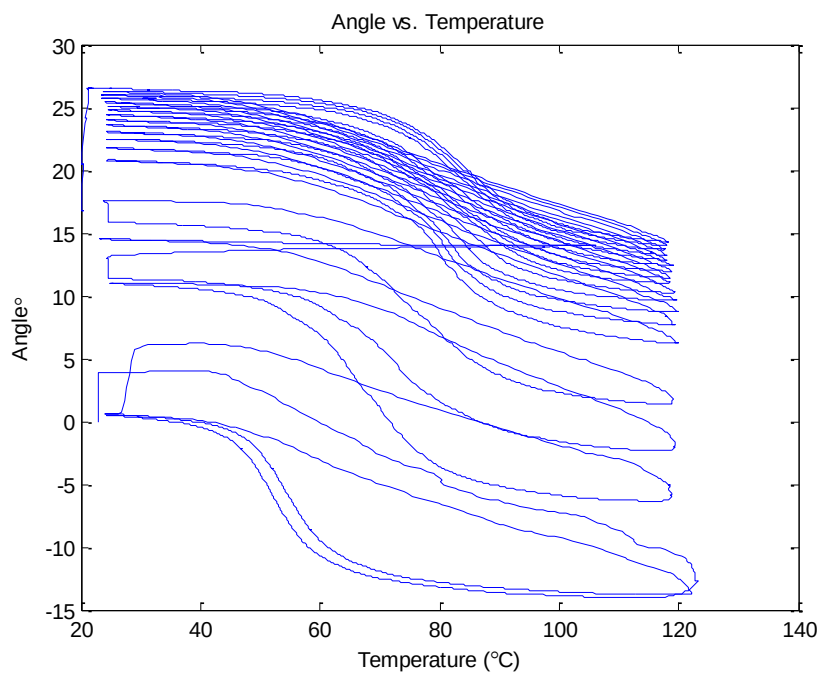

Figure 18: TIG 1 Angle vs. Temperature

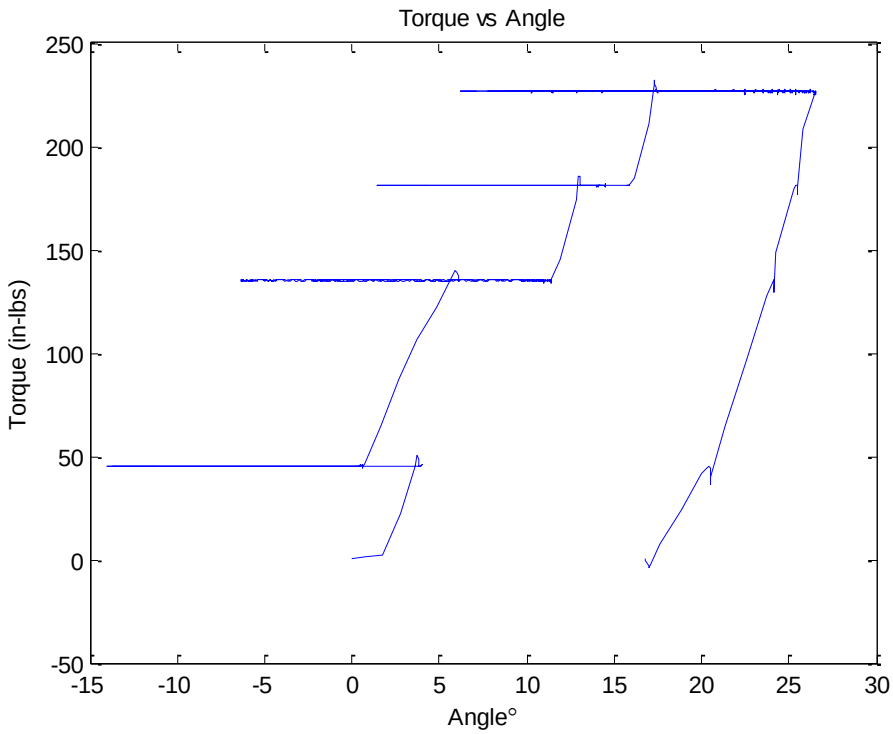

Figure 19: TIG 1 Torque vs. Angle

The results of the second test for the TIG 1 specimen were shown first because they best represent the data being produced. The initial tests for the TIG 1 and TIG 2 specimens show all of the same physical trends, but an extra influence on the system was unintentionally added. The unintentional influence came from the right grip slipping because of the lamination melting between the aluminum shims in the right grip. This slipping skewed the angular deflection data in a nonlinear trend with extra deflection being added during increases of torque as seen in Figures 20 and 21. This problem was addressed in the rig improvements, Section 2.2. While the grip was slipping, the motor control was able to compensate for the slipping to apply a constant torque. While the angular deflection data is not particularly useful it is safe to say that the TIG welded joints held up to thermal cycling under a constant torque without showing any signs of weakness. Table 7 shows the important fact that none of the TIG testing resulted in a failed joint.

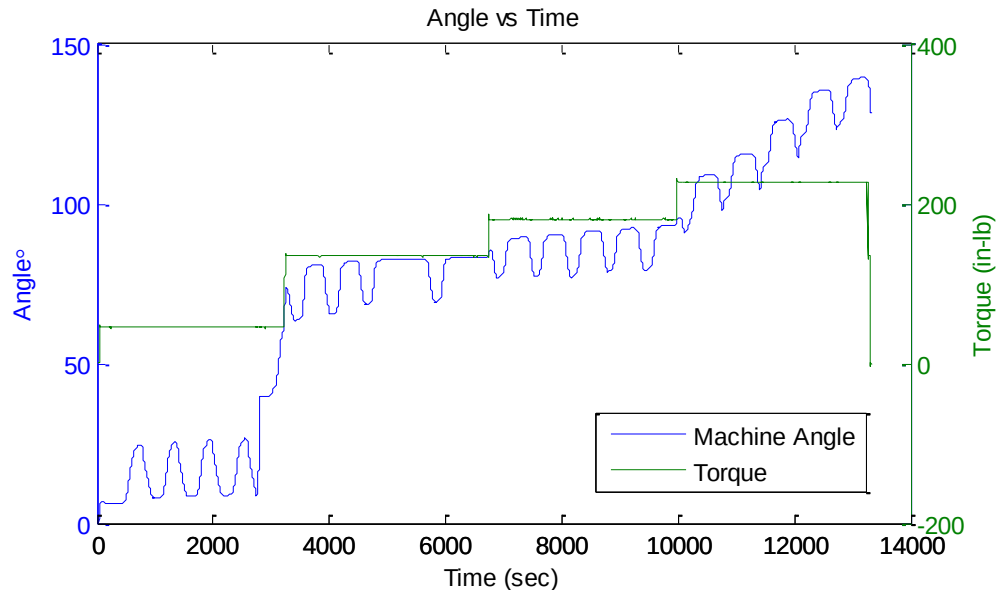

Figure 20: TIG 1 First Test Angle and Torque vs. Time

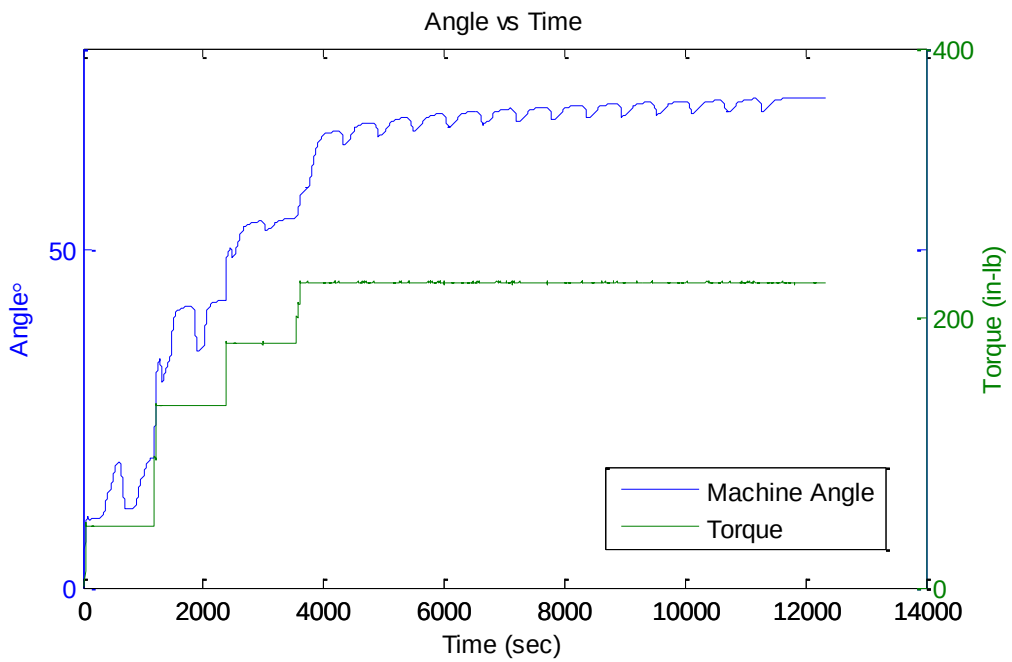

Figure 21: TIG 2 Angle and Torque vs. Time

The shear stresses in the NiTi tubes were approximated by finding the maximum shear stress in the tube by using the outer and inner radius and the torque. Equations iii and iv show the equations used to find the shear stress in the TIG welded joints.

$$\tau = \frac{T * r}{J} \qquad (iii)$$

$$Where: \tau = Shear\ Stress(psi), T = Torque(ksi), r = Outside\ tube\ radius\ (in)$$

$$and\ J\ is\ the\ polar\ moment\ of\ inertia$$

$$J = \pi * \frac{OD^4 - ID^4}{32} \qquad (iv)$$

$$Where\ OD = outside\ diameter\ of\ the\ tube, ID = inside\ diameter\ of\ the\ tube$$

Table 7: TIG Results Summary

Specimen #	Cycling Temperatures	Torque in-lb (Nm)	Shear Stress Ksi (MPa)	Failing Point (Time or Cycles)
TIG1	Cycled	Step Increments	Step Increments	N/A
TIG2				
TIG1	70F to 250F (25C to 121C)	45.1 (5.10) to 226.5 (25.6)	5.00 (34.5) to 25.1 (173)	

4.3 Discussion

The TIG welds have held up under endurance tests and showed no sign of weakness. The right grip was rotating relative to the input shaft, which makes the angular deflection data of little value in the first two tests. However the motor controller was able to compensate for the slipping and kept a constant load on the joint throughout the thermal cycling tests. The second time the TIG 1 specimen was tested the right grip was corrected and the angular data clearly shows the properties of an effective actuator. In Figure 17 it can be seen that the average value of the angular deflection is growing. This is because of creep in the NiTi, which is a concern being addressed by Boeing [5]. This creep is thought to be eliminated after extensive thermo-mechanical cycles.

CHAPTER 5: CONCLUSIONS AND FUTURE WORK

The testing accomplished in this portion of the project points to TIG as a promising bonding process which merits additional testing. The second round of adhesive testing did not give positive results for the use of adhesives in application because of serious problems in their endurance. However, adhesive batch differences could be considered. The TIG welded specimens performed well in thermal cycling and look to provide a promising long term solution for joining NiTi to structural materials. A further investigation of TIG welding with a significant number of specimens looks to be the next step in the process of finding ways to utilize NiTi as a solid state actuator. Factors influencing the formation of the TIG weld could be studied in an effort to create the strongest weld possible. These factors include the thickness of the Ni rich filler, the outer and inner diameters of the Ni filler, and the heat treatment of the structural material being joined with the NiTi.

BIBLIOGRAPHY

1. Dapino, M., and Fox, G., and Hahnlen, R. “TIG Welding of Nickel-Titanium to 304 Stainless Steel” ASME SMASIS 2011 Conference, Sept. 18-21, 2011
2. Dapino, M., and Fox, G. “Joining of Shape Memory Alloys and Structural Materials” SVC Meeting, The Ohio State University, 10-11 Aug. 2011
3. Dapino, M., and Hahnlen, R. “Development and Characterization of NiTi Joining Methods and Metal Matrix Composite Transducers with Embedded NiTi by Ultrasonic Consolidation” M.S. Thesis 2009.
4. Dapino, M., and Fox, G. “Design and Analysis of Joints Between Shape-Memory NiTi Torque Tubes and Structural Materials” M.S. Thesis Apr. 2012
5. Mabe, James. Ruggeri, Robert. Rosenzweig, Ed. Yu, Chin-Jye (Mike). *NiTinol Performance Characterization and Rotary Actuator Design.* Boeing Phantom Works. 2004.

APPENDIX

Ultimate Failure Torque Plots

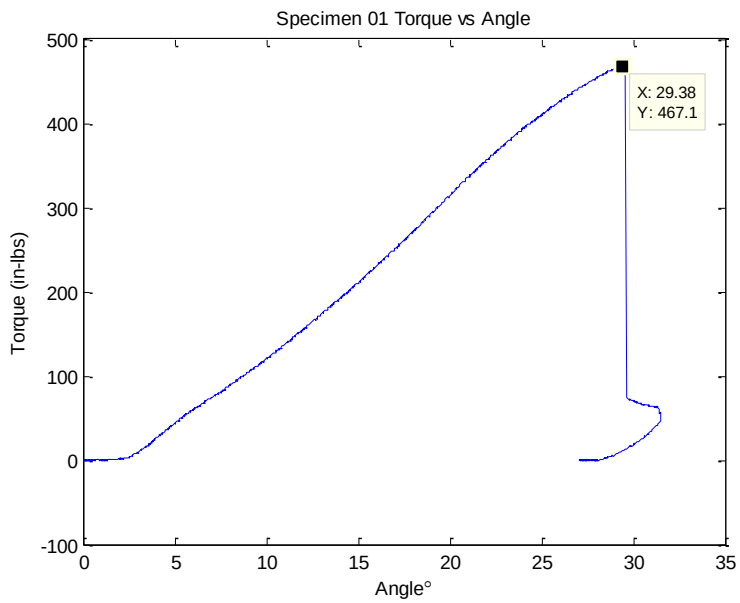

Figure 22: Torque vs. Angle for Specimen 01

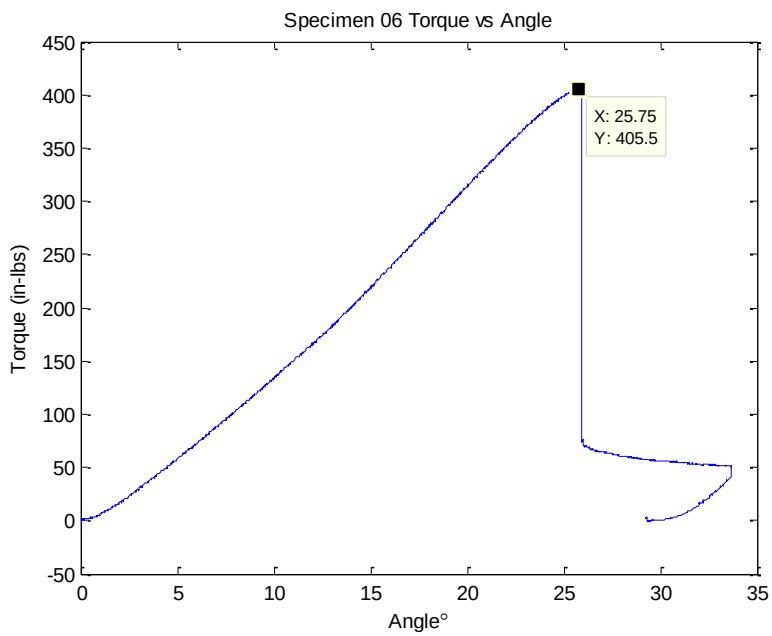

Figure 23: Torque vs. Angle for Specimen 06

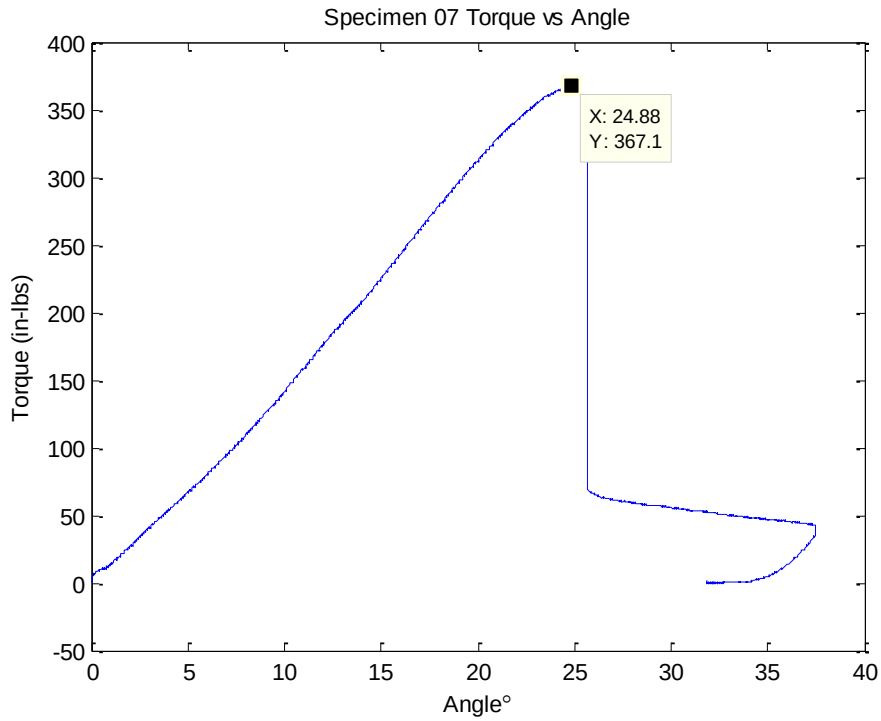

Figure 24: Torque vs. Angle for Specimen 07

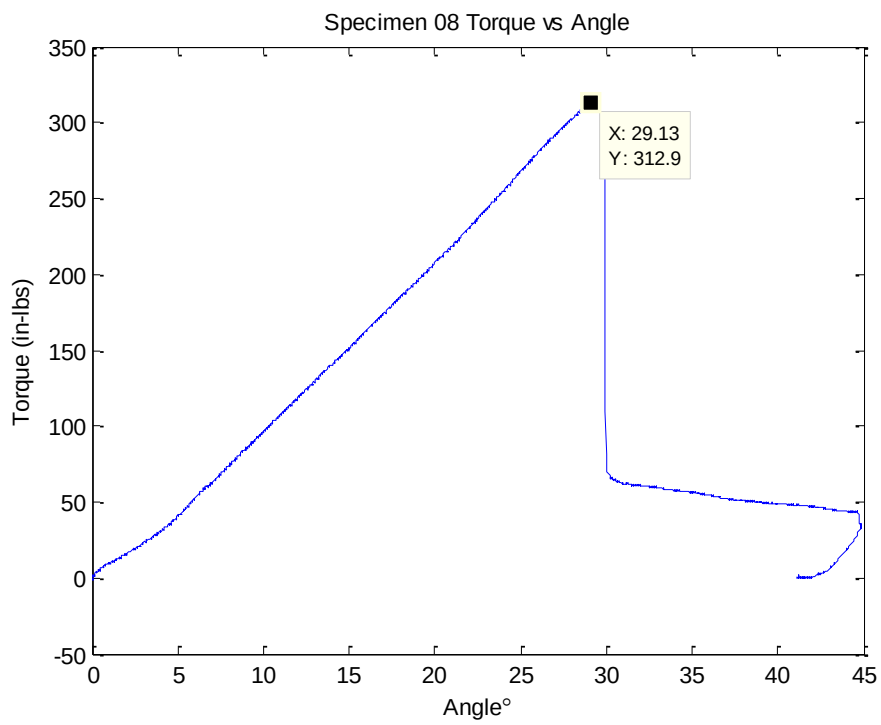

Figure 25: Torque vs. Angle for Specimen 08

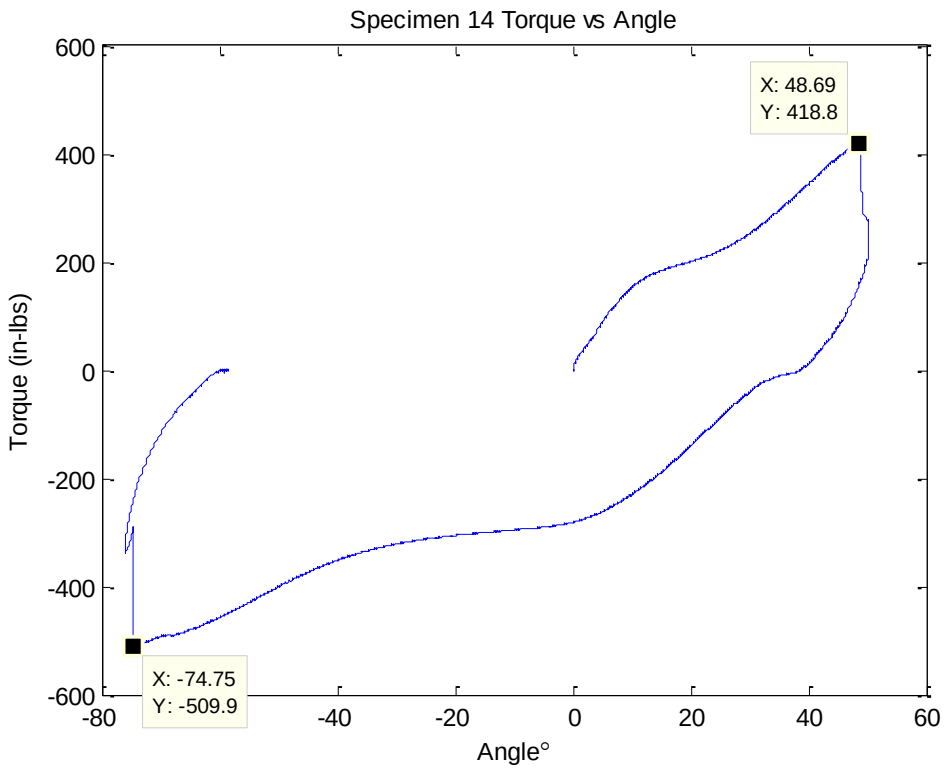

Figure 26: Torque vs. Angle for Specimen 14

Adhesive Creep Tests

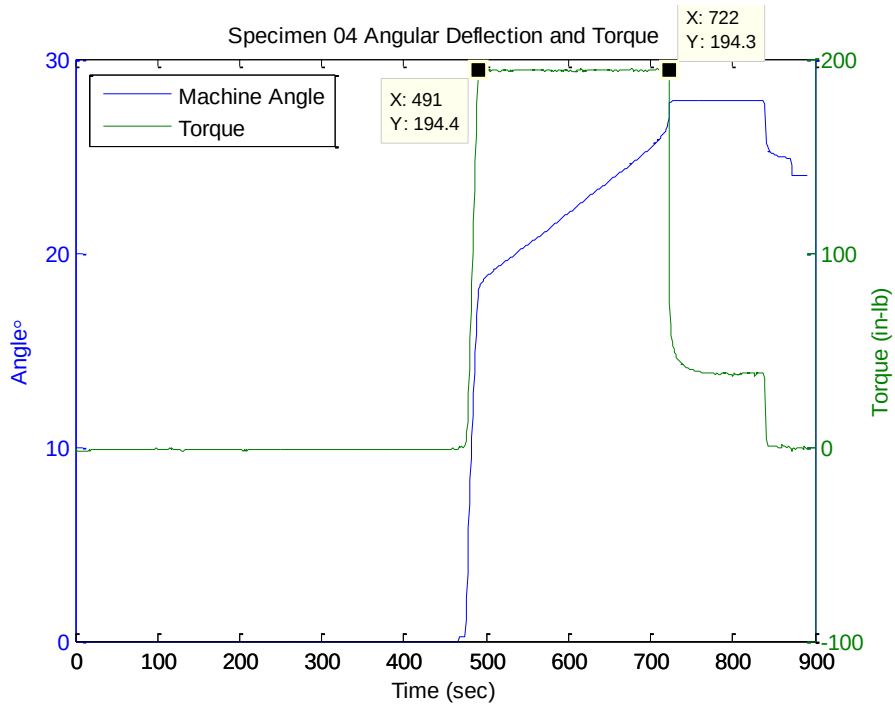

Figure 27: Angular Deflection and Torque for Specimen 04

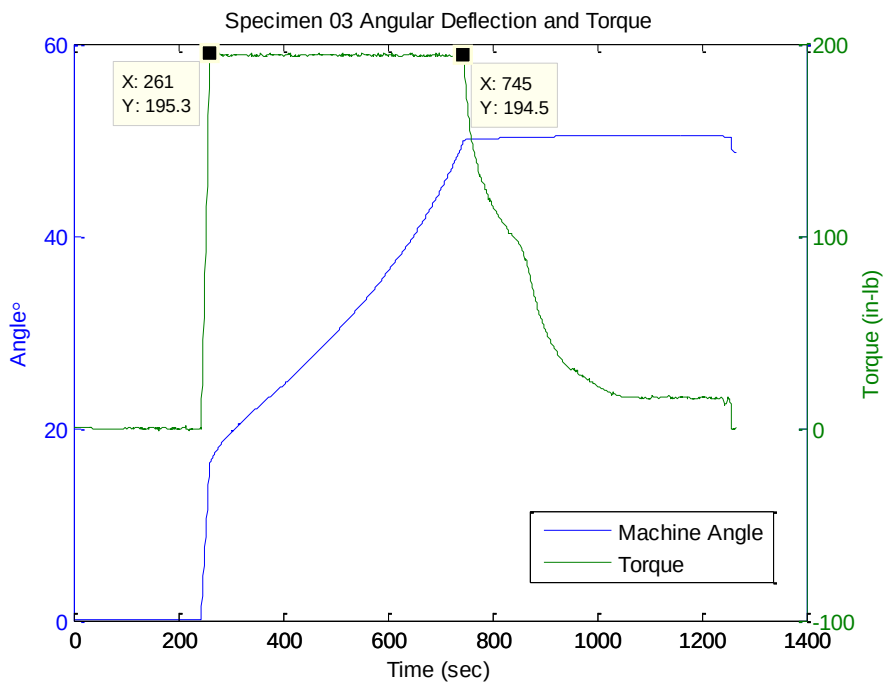

Figure 28: Angular Deflection and Torque for Specimen 03

Adhesive Thermal Cycling

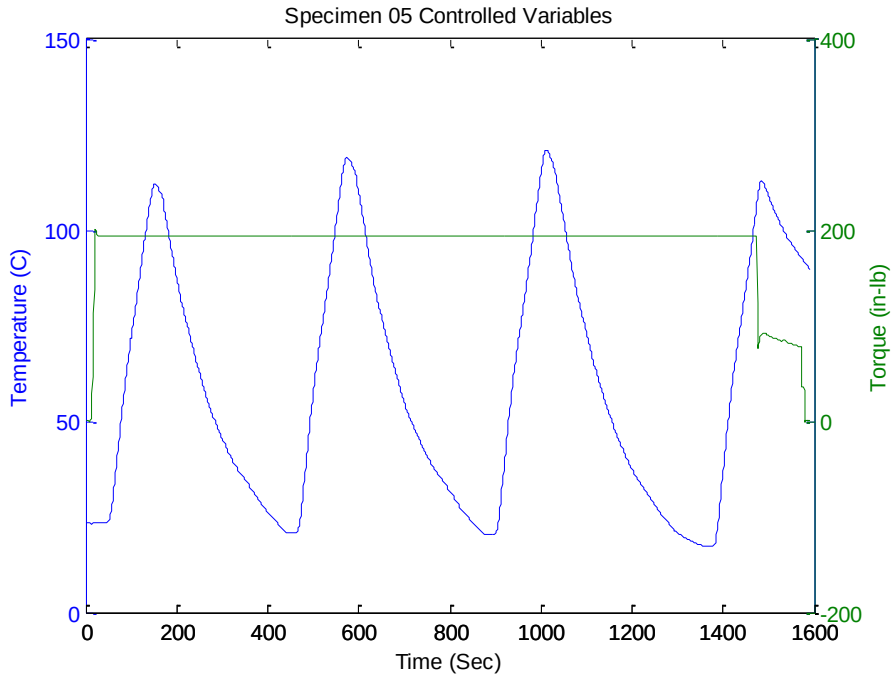

Figure 29: Controlled Variables Specimen 05

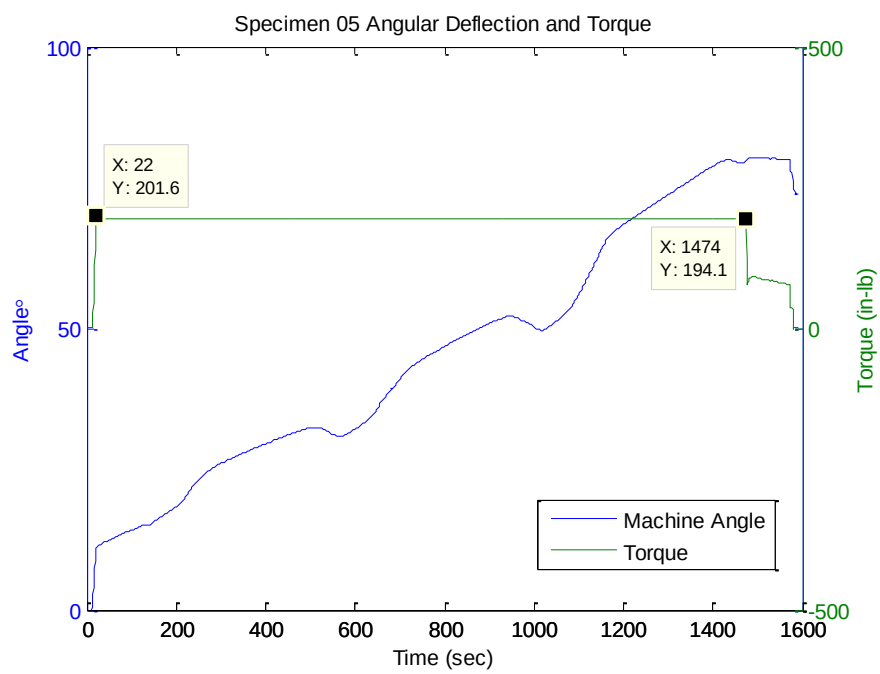

Figure 30: Angular Deflection and Torque for Specimen 05

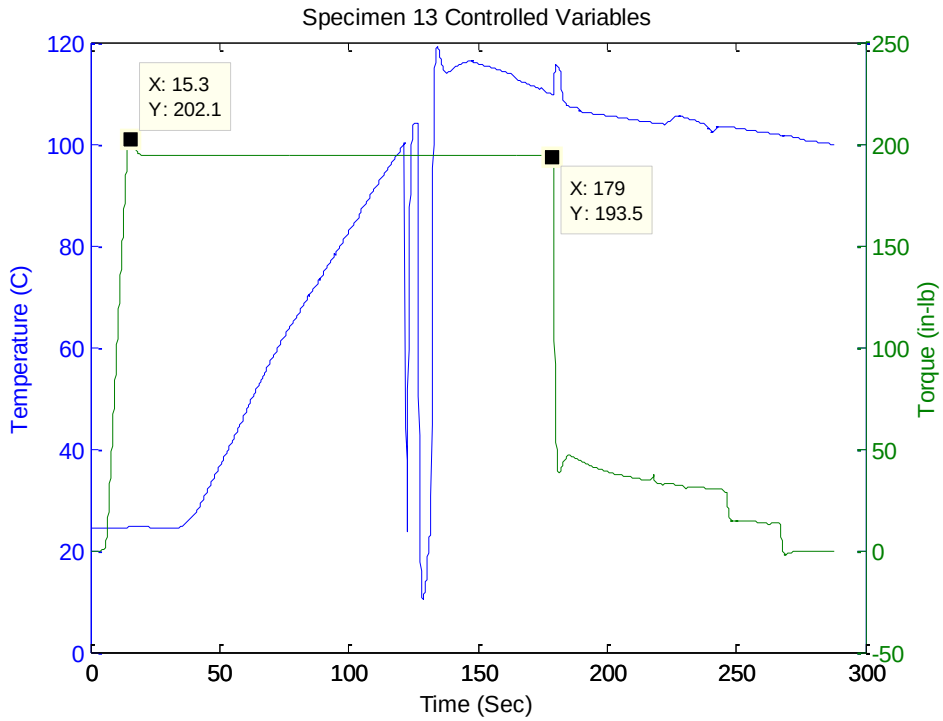

Figure 31: Controlled Variables Specimen 13

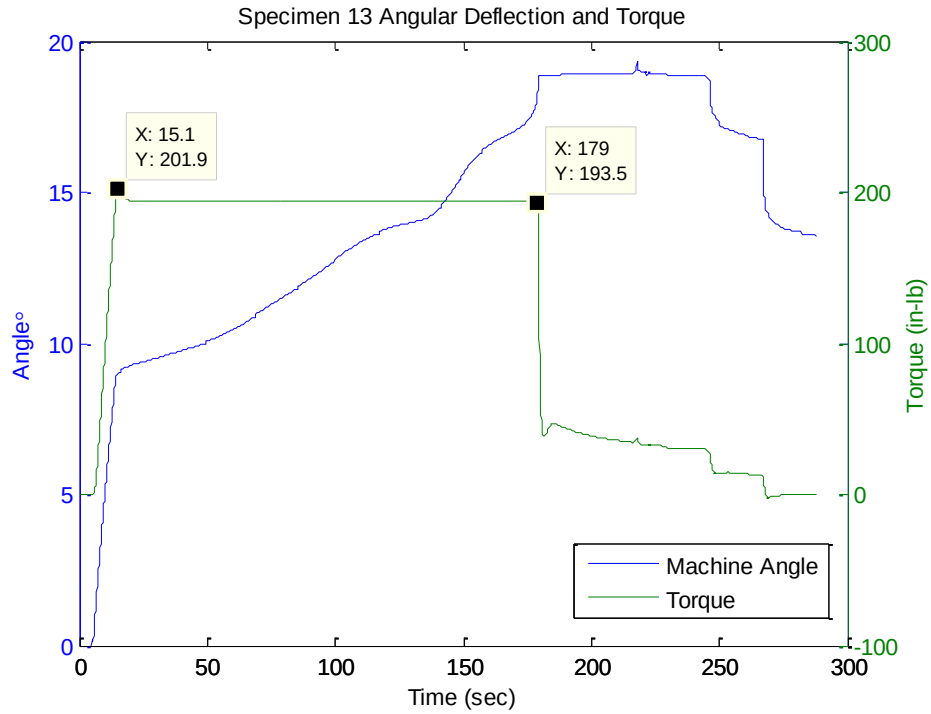

Figure 32: Angular Deflection and Torque for Specimen 13